Optimization of TIG Welding Parameters for Ti-6Al-4V Titanium Alloy using the Taguchi Design of Experiment

Abdul Sattar[1], Azhar Hussain[1], Musharaf Abbas[2], Muhammad Nadeem Azam[1], Kashif Mehmood[3], Aneela Wakeel[1], Sarim Ali[1],

[1.] Department of Metallurgy and Materials Engineering, University of Engineering and Technology Taxila, Pakistan
[2.]School of Materials Science & Engineering, University of New South Wales, Sydney, NSW 2052, Australia
[3]School of Chemical and Materials Engineering (SCME), National University of Science and Technology, Islamabad, Pakistan.
Received: 13-11-2022, Received in Revised form: 05-12-2022, Accepted: 16-12-2022, Published: 31-12-2022

Abstract

This paper presents the effect of tungsten inert gas welding parameters (i.e. welding current, welding speed and filler wire speed) on weld bead geometry, notch tensile strength (NTS) and weld bead hardness of 2.0 mm thick annealed Ti6Al4V titanium alloy sheet welded in a square butt joint configuration using Taguchi L9 (3^3) three level - three factor matrix. Taguchi's signal to noise ratios was calculated to obtain optimum welding parameters for Vickers hardness at weld area, Notch tensile strength (NTS), Front bead width (FBW) and Front reinforcement height (FRH). Analysis of Variance (ANOVA) was conducted to find statistically significant and insignificant factors with respect to each response. It was noted that welding speed has significant effect on weld hardness, notch tensile strength, front bead width and height. Optimum parameters for hardness were found to be 120A current, 400 mm / min welding speed and 250mm/min filler wire speed. Confirmation test using the optimal levels of welding parameters was also conducted in order to compare predicted results with values obtained through experimentation.

Keywords: Ti6Al4V; Tungsten inert gas welding; Taguchi, L9 (3^3); ANOVA; S/N ratio.

Introduction

Titanium alloys are being generally used in aerospace, medicinal, chemical, automotive, petrochemical, nuclear and power generation industries due to very good high temperature properties, high specific strength, excellent weldability, good corrosion resistance, low coefficient of thermal expansion and excellent biocompatibility. Titanium is an allotropic element which exhibit more than one crystallographic form. At room temperature, pure elemental titanium possesses a hexagonally close packed (hcp) crystal structure which is termed as alpha (α) phase. When temperature rises above 882°C, this transforms to a ductile body centred cubic (bcc) crystal structure, known as beta (β) phase. Titanium alloys are classified into three major categories such as α alloy, β alloy and α + β alloys. [1]

Two phases alloys like α+β, are presently the most common in all types of titanium alloys as physical as well as mechanical properties of these alloys can be easily optimized by either changing the chemical composition or controlling the micro structural phases during processing [2-3]. Ti64 (Grade-5) is a typical alpha + beta titanium alloy consisting of mixture of two phases α and β, with volume fraction of about 65% and 35% respectively. The β transition temperature of this alloy generally lies between 975 °C and 1015 °C. It varies with its percentage alloying elements, presence of interstitial element, and change in cooling rate [4]. Ti6Al4V alloy has significant applications in aerospace industry due to combination of excellent properties like heat resistance, good weldability, high specific strength and high toughness [5]. Ti6Al4V is the most frequently used alloy, over 70% of all titanium alloys being used in different sectors.

In the recent past, electron beam welding [6,7], laser beam welding [8-10], and arc welding processes like tungsten inert gas and plasma welding [11,12] have been used to weld titanium alloy parts. While it is well known that the beam welding processes like laser and electron beam welding can yield high quality, these processes pose high capital and running costs. Tungsten inert gas (TIG) arc welding, on the other hand, is widely employed technique used in aerospace and other engineering industries owing to its cost effective use. In this process an arc is being generated between tungsten electrode and the weld specimen in an inert atmosphere. The shielding gas, such as argon, helium or mixture of both, serves as medium of electron transport and protects the hot tungsten electrode and weld metal from oxidation. This process produces high quality, clean welds, allows operator to easily control the process, however high heat input involved in this process generates defects in weld area and hence mechanical strength may be compromised. Mechanical properties of welds especially in thin sheets of titanium alloys depend on geometry of weld bead, grain size, type of phases and their distribution in weld and heat affected zones. In order to control the strength performance of the weld, attention is now being given to control weld bead geometry through optimization techniques.

In this regard Nazmul Huda et al. investigated the effect of TIG welding parameters on weld profile of 1.0 mm thick Ti6Al4V and Ti3Al2.5V titanium alloys by applying L9 Taguchi technique, they showed that at optimal welding conditions, welding current and welding speed are major influencing factors that control bead width and penetration [13]. Akbari et al. analysed temperature distribution and weld pool profile like bead depth and bead width on 3.0 mm thick Ti6Al4V plate by using Nd; YAG laser welding [14]. Omoniyi et al. studied the effect of laser power and welding speed parameters through Taguchi L9 (32) design of experiment, on the tensile, micro hardness, and microstructure of Ti6Al4V alloy. They found that the micro hardness is maximum at the weld zone and decreases towards the base metal [15]. M. Balasubramanian et al [16] investigated the effect of pulsed current tungsten inert gas welding parameters on 1.6 mm thick Ti6Al4V alloy by using L16 modified Taguchi technique, with a purpose to improve notch tensile strength, yield strength and tensile strength. Experimental results coupled with ANOVA proved that pulse frequency is the most influencing parameters for all the responses. Khattar Ajit et. al [17]developed mathematical

https://doi.org/10.24949/njes.v15i2.731

model using three factor, three levels, Taguchi L9 design to improve weld bead strength of 304 austenitic stainless steel.
Juang and Tarng [18] applied modified L16 Taguchi orthogonal array for selection of appropriate TIG welding factors for controlling weld pool geometry (i.e. front height, back height, front width and back width) of stainless steel plate having thickness of 1.50 mm. Pasupathy.J and Ravisankar.V [19] performed tungsten inert gas welding between low carbon steel and aluminium plate, by using L9 Taguchi technique with an aim to improve weld strength. The welding characteristics of dissimilar joints were analysed using signal to noise ratio and analysis of variance. Dongxia et al. [20]applied the Taguchi L9 technique for laser welding of Al-Mg alloy. They selected parameters like laser power, welding speed and wire feed rate. Experimental results, indicates that the welding speed and filler wire rate has significant effect on weld bead geometry. Results showed that with the increase of welding speed, reduction in front bead width observed and increase of wire feed rate resulted in larger front bead width
In this research tungsten inert gas welding was performed on 2.0 mm mill annealed Ti6Al4V titanium alloy sheet by employing Taguchi's L9 orthogonal array. Effect of welding factors like current, welding speed and filler wire rate on weld hardness, notch tensile strength and weld bead geometry was investigated. After welding, signal-to-noise ratio and analysis of variance was conducted to determine optimal levels and contribution of each factor towards response values. Confirmation test was also performed to compare predicted results with experimental results.

Taguchi Philosophy

Taguchi proposed a special design of experiment which utilizes orthogonal arrays to study entire set of parameters with a minimum number of experiments only. The values of quality characteristics obtained through this experimentation are transformed to signal to noise S/N ratio [21].
Signal to noise ratio in Taguchi method is usually used to identify control factors by reducing variability in the process. The term, "signal" implies the mean value while "noise" indicates the standard deviation term. It means that lower variability in the process is ensured through maximizing the *S*/*N* ratio. However, depending on the type of response desired, Taguchi classified *S*/*N* ratios into three categories: nominal the better, larger the better and smaller the better [22]. For optimization, Taguchi's methodology can be divided into four stages, which are planning, performing the experiment, checking and validation. Step wise procedure for optimization of any process is given in Fig.1. [23-25]. For a particular response, a higher signal to noise ratio indicates a better quality characteristic, regardless of the quality parameters opted for a particular response. The S/N ratio can be determined from Eq. 1-3. [26].

Smaller is the better: This is used where the smaller value is desirable

$$\frac{S}{N} = -10\log_{10}\left(\frac{1}{n}\sum_{k=1}^{n} y_i^2\right) \quad \text{Eq. 1}$$

Larger is the better: This is used where larger value is desirable.

$$\frac{S}{N} = -10\log_{10}\left(\frac{1}{n}\sum_{k=1}^{n} \frac{1}{y_i^2}\right) \quad \text{Eq. 2}$$

Nominal is the better: This is used where targeted or nominal value is desirable

$$\frac{S}{N} = -10\log_{10}\left(\frac{1}{n}\sum_{k=1}^{n} \frac{\mu^2}{\sigma^2}\right) \quad \text{Eq. 3}$$

Where μ = mean or targeted value , (1/n) $\sum_{k=1}^{n} y_i$; σ^2 = variance, summation of square of difference between observed and targeted value divided by degree of freedom which is equal to = (1/n-1) $\sum_{k=1}^{n}(y_i - \mu)^2$ and"y_i" represents quality characteristic or response value of ith trial. and "n" denotes number of replications for the same experiment.
Analysis of variance (ANOVA) is a satisfactory technique that establish the degree of difference or similarity between two or more groups. The purpose of this test is to identify parameters that significantly affects the performance characteristics. This is accomplished by splitting the total variability or total sum of squares (SST) into sum of squares between (SSB) and sum of squares within each group (SSW) These values can be measured from Eq. 4-6.

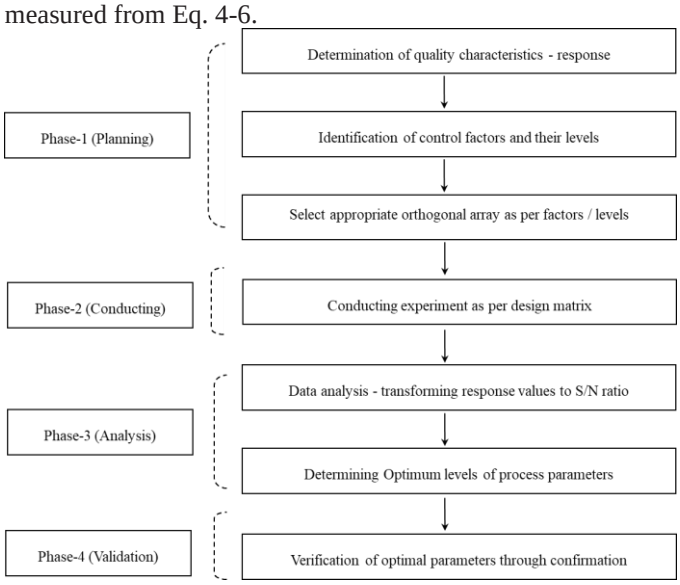

Fig. 1 Flow chart representing the Taguchi method of optimization

$$\text{SST (Sum of squares total)} = \sum_{i=1}^{k}\sum_{j=1}^{m}(y_{ij} - \bar{y})^2 \quad \text{Eq. 4}$$

$$\text{SSB (Sum of squares between)} = n\sum_{i=1}^{k}(\bar{y}_i - \bar{y})^2 \quad \text{Eq. 5}$$

SSW (Sum of squares within) Eq. 6

$$= \sum_{i=1}^{k} \sum_{j=1}^{m} (y_{ij} - \bar{y}_i)^2$$

Where, SST is total sum of squared deviation, SSB is a sum of squared deviation between group, also called sum of squares for treatment or parameter. SSW is a sum of squared deviation within each group also called sum of squares for residuals error (SSE). y_{ij} represents ith observation in a group (e.g. y_{13} is the third observation in first group while y_{21} is the first observation in second group), $\bar{y}_i$ indicates group mean, k indicates number of groups in a matrix, in our case number of groups are 3, $\bar{y}$ indicates grand mean or over all mean of all observations. m represents number of observations in each group.

Experimental Work

Tungsten inert gas (TIG) welding was conducted on 2.0 mm thick mill annealed Ti6Al4V titanium sheet in a square butt joint configuration in a single pass by using semi-automatic Lincoln-375 machine equipped with trailing and purging gas facility. Sketches of plates before and after welding are shown in Fig-2. The chemical composition of parent metal and filler wire was analysed through spark emission spectrometer is shown in Table-1; physical & mechanical properties of parent metal are given in Table 2-3. Three in put factors, welding current, welding speed and filler wire rate and four response factors like hardness, notch tensile strength, front bead width and front bead height have been identified after literature review. Typical weld pool geometry indicating front bead width and front bead height is shown in Fig-3. Particular process parameters and their respective levels are presented in Table-4. Nine experimental runs with one repetition were conducted as per Taguchi's L9 (3^3) orthogonal array [27-29]. For this titanium plates of 2.0 mm thickness were cut into the required sizes of 120 mm by 350 mm by shearing machine, and edges were machined by carbide end mill cutter on milling machine. The burr from cutting edges of plates were removed by manual filing. Before welding all the plates were cleaned by stainless steel brush and picked by chemical solution containing hydrofluoric (5% by volume) and nitric acid (35% by volume) followed by water rinse and air drying. The plates to be welded were placed on a copper bar containing holes of diameter 1.0 mm for passage of back shielding gas, the ends of sheets were clamped to maintain the alignment and uniform distance of 0.2 mm between weld edges. The argon gas with purity 99.990% was used as a shielding for primary, back and trailing to avoid excessive oxidation reaction with titanium during welding. Constant welding parameters used during welding are given in Table -5.

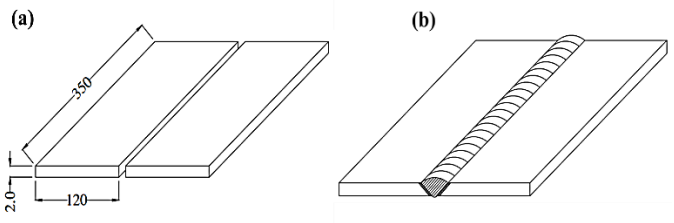

Fig. 2 Schematic representation of Ti6Al4V plates (a) before welding (b) after welding

After welding the samples for hardness and notch tensile strength, were cut through electric discharge machine. For hardness the specimens were mechanically grinded, polished with aluminium oxide and diamond paste. After polishing the specimens were macro- etched by using Kroll's solution (3% HF+5% HNO_3+92 %H_2O) for 2 minutes to reveal important features of weld bead geometry. Coarse grain structure observed in the specimens having high current and low welding speed parameters and vice versa. The hardness was measured at 5kgf load using low Vickers hardness testing machine (Model HV5), and same specimens were utilized for measurement of weld bead geometry on optical microscope. For notch tensile strength double edge notched specimens, were machined through electric discharge machine. U type notches (depth 5.0 mm, root radius 1.0 mm) were incorporated at the centre of weld line to ensure crack propagation along the weld centreline during tensile testing. Notch tensile test was carried out at a constant displacement speed of 3.0 mm/min. Specimens used for hardness and NTS are shown in Fig-4-5.

Table 1: Chemical composition of base plate and filler metal (wt%)

Material	Al	V	Fe	C	O	Ti
Parent Plate	5.56	3.72	0.04	0.03	0.002	90.40
Filler wire	5.76	3.60	0.25	0.05	0.003	90.20
Standard ASTM B 265	5.5-6.75	3.50 - 4.50	0.40 max	0.08 max	0.20 max	balance

Table 2: Physical properties of Ti6Al4V

Density, g/cm^3	Specific heat JKg^{-1}K^{-1}	Melting point, ^{o}C	Thermal conductivity, W/mK	Electrical resistivity, Ω-mm^2/m	Young's Modulus GPa	Thermal expansion µm/m-k
4.43	610	1660	6.7	168	114	8.6

Table 3: Mechanical properties of base metal

Properties	Yield strength (MPa)	Tensile Strength (MPa)	% elongation	Hardness (HV5)
Actual	950	990	12	310
Standard ASTM B265	≥ 828	≥ 895	≥ 10	--

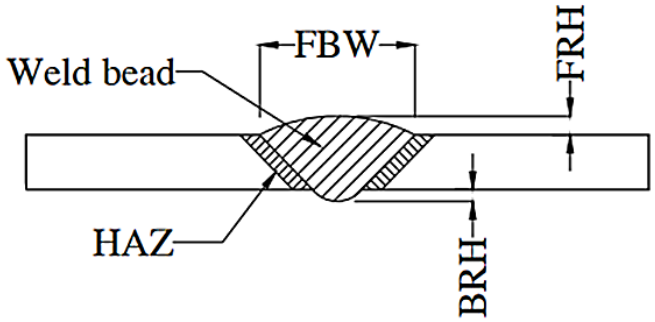

Fig. 3 Nomenclature of weld bead

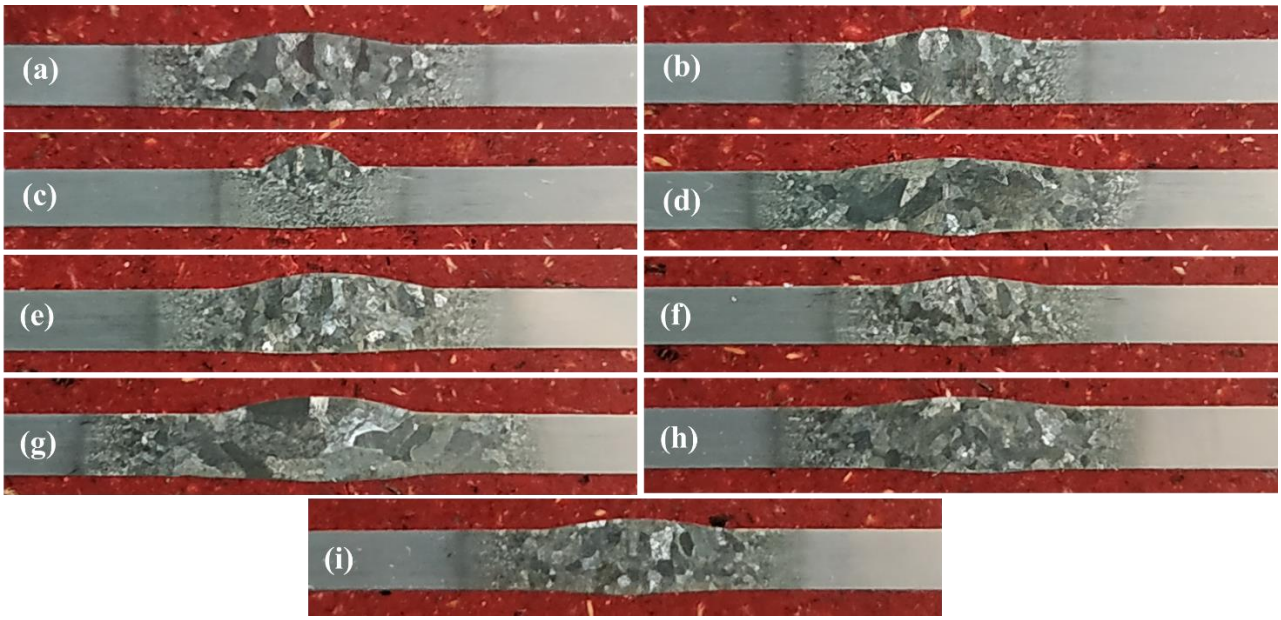

Fig. 4 Macrostructure of welded plates (specimens a to i represents welded plates of experiment 1 to 9)

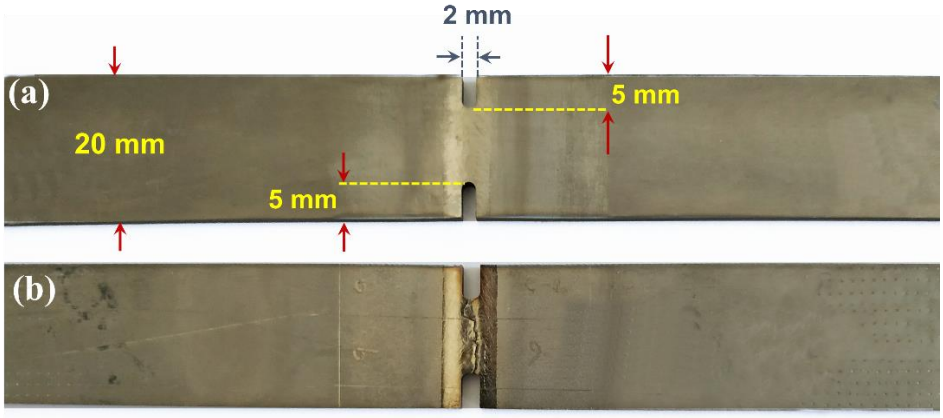

Fig. 5 Notch tensile specimen (a) before breakage, (b) after breakage

Table 4: Welding parameters and their levels

Welding parameters	Symbol/Code	Units	Levels		
			1	2	3
Welding current	A	amp	100	125	150
Welding speed	B	mm/min	200	300	400
Filler wire speed	C	mm/min	150	250	350

Table 5: Constant welding parameters

Process parameters	Constant Value	Process parameters	Constant Value
Filler wire diameter	1.60 mm	Primary gas flow rate	14-16 liter/min
Tungsten electrode diameter	2.0 mm	Trailing gas flow rate	10-12 liter/min
Protecting gas	Ar 99.99%	Back gas flow rate	10-12 liter /min
Tungsten tapper length	4.0 mm	Pre and post flow time	20-25 seconds
Voltage	11 ± 0.5 V	Shielding Cup size	12 No (19 mm)

Results and discussion

A Taguchi robust design was employed to determine the optimal conditions and to identify welding parameters which influence greatly on responses like hardness, notch tensile strength, front bead width and front bead height. In this study a higher weld bead hardness and notch tensile strength is desirable to enhance welding strength, hence statistical analysis is carried out with larger the better, and for FBW and FBH smaller the better criteria were applied. The mean values of hardness, front bead width (FBW) and front bead height (FBH) of each experimental run are presented at Table-6 and signal to noise ratios calculated from Eq.1-2 are shown in Table-7. The mean S/N ratio for each level of welding parameters were calculated by adding S/N ratio of corresponding level and then dividing this value by number of observations. For example, the mean S/N ratio of factor C (filler wire speed) for front bead height at level 2 is calculated as (5.193+4.731+6.936)/3, which is equal to 5.620. The average S/N ratios for each level of other welding parameters commuted in similar manner are summarized at Table-8. Main effect plots of S/N ratios for hardness, notch tensile strength, front bead width and front bead height are shown in Fig-6. A higher signal to noise ratio indicates better performance and the corresponding level is called optimal level. The delta value was determined by subtracting the lowest value from highest value in each group. Higher delta reflects greater impact on responses. Based on the result of mean S/N ratios, the optimal conditions for maximizing the hardness are A2B3C3, welding current at level 2 (125A), welding speed at level-3 (400mm/min) and wire feed speed at level 3 (350mm/min). As per Fig.6 a), weld hardness increases as the current increases, however further increase in current reduces hardness and this might be due to coarsening of grain size associated with higher heat input. The increase of welding speed causes increase in hardness, this might be due to faster cooling rate and low heat input values. Similar trend for increase in weld hardness with welding speed is also reported at [29].

Optimal condition for notch tensile strength are A3B1C2, welding current at level 3 (150 A), welding speed at level 1 (200 mm/min) and filler wire rate at level 2 (250 mm/min). As the value of current increases notch tensile strength increases and as the value of welding speed increases from level-1 to level -3 the notch tensile strength decreases. This might be due to insufficient heat input that required to properly fuse or melt the edges. Main effects plot for notch tensile strength are shown in Fig. 6b). Scanning electron microscopy (JEOL JSM 6490LV) was conducted to analyse surface morphology of broken notch tensile specimens. Low notch tensile strength observed in the plates having lack of penetration and porosity in the weld area. The cross sectional SEM micrographs of fracture surfaces of notch tensile specimens are presented in Fig 7~9.

Optimal conditions for front bead width (FBW) are, welding current at level-1 (100A), welding speed at (400mm/min) and filler wire rate at (250mm/min). As the welding current decreases the front bead width also decreases and vice versa. Similar trend for increase in bead width with high welding currents are also reported at [30,31]. Optimal conditions for front bead height (FBH) are welding current at level-3, welding speed at level-2 and wire feed rate at level-1.

Table 6: Experimental design using Taguchi's L9 (3^3) orthogonal array and results

Exp. no	Factors			Hardness HV	NTS MPa	FBW mm	FBH, mm
	A	B	C				
1	100	200	150	311	1166	6.20	0.60
2	100	300	250	319	1020	5.40	0.55
3	100	400	350	330	650	4.50	0.70
4	125	200	250	318	1259	8.80	0.58
5	125	300	350	331	1056	7.60	0.51
6	125	400	150	338	700	6.30	0.40
7	150	200	350	320	1310	11.30	0.70
8	150	300	150	327	1220	9.30	0.37
9	150	400	250	330	1090	7.43	0.45

Table 7: S/N ratios of experimental results

Exp. no	S/N ratios (dB)			
	Hardness	NTS	FBW	FBH
1	49.86	61.35	-15.85	4.437
2	50.08	60.17	-14.66	5.193
3	50.37	56.38	-13.07	3.098
4	50.05	62.00	-18.89	4.731
5	50.40	60.48	-17.63	5.849
6	50.58	56.90	-16.00	7.959
7	50.10	62.34	-21.07	3.098
8	50.29	61.73	-19.37	8.636
9	50.37	60.75	-17.43	6.936

The analysis of variance (ANOVA) was used to analyse the effect of welding parameters on hardness, notch tensile strength, FBW and FBH. Results of total sum of squares and sum of squares between groups were calculated through Eq. 4-5, and results are summarized at Table 9-12. Percent contribution is the ratio of sum of squares between to total sum of squares. In the table-8, welding speed is found to be the most significant factor affecting weld bead hardness with contribution about 71.32 % followed by welding current by 21.98% and filler wire rate by 5.0%. A factor is considered to be significant if P-value is less than 0.05. Statistically, there is a tool called F test, named after Fisher, and used to identify parameters that have significant effect on the quality characteristic or response values. In the analysis, F-ratio is a ratio of the mean square of parameters to mean square due to error. For hardness, F value for factor A, B and C are 28.88, 93.70 and 7.81 respectively. P values for factor A and B are 0.033 and 0.010 respectively, which means that both factors are significant, while P value for factor C is 0.133 which is insignificant. The interaction of factors was neglected in this study.

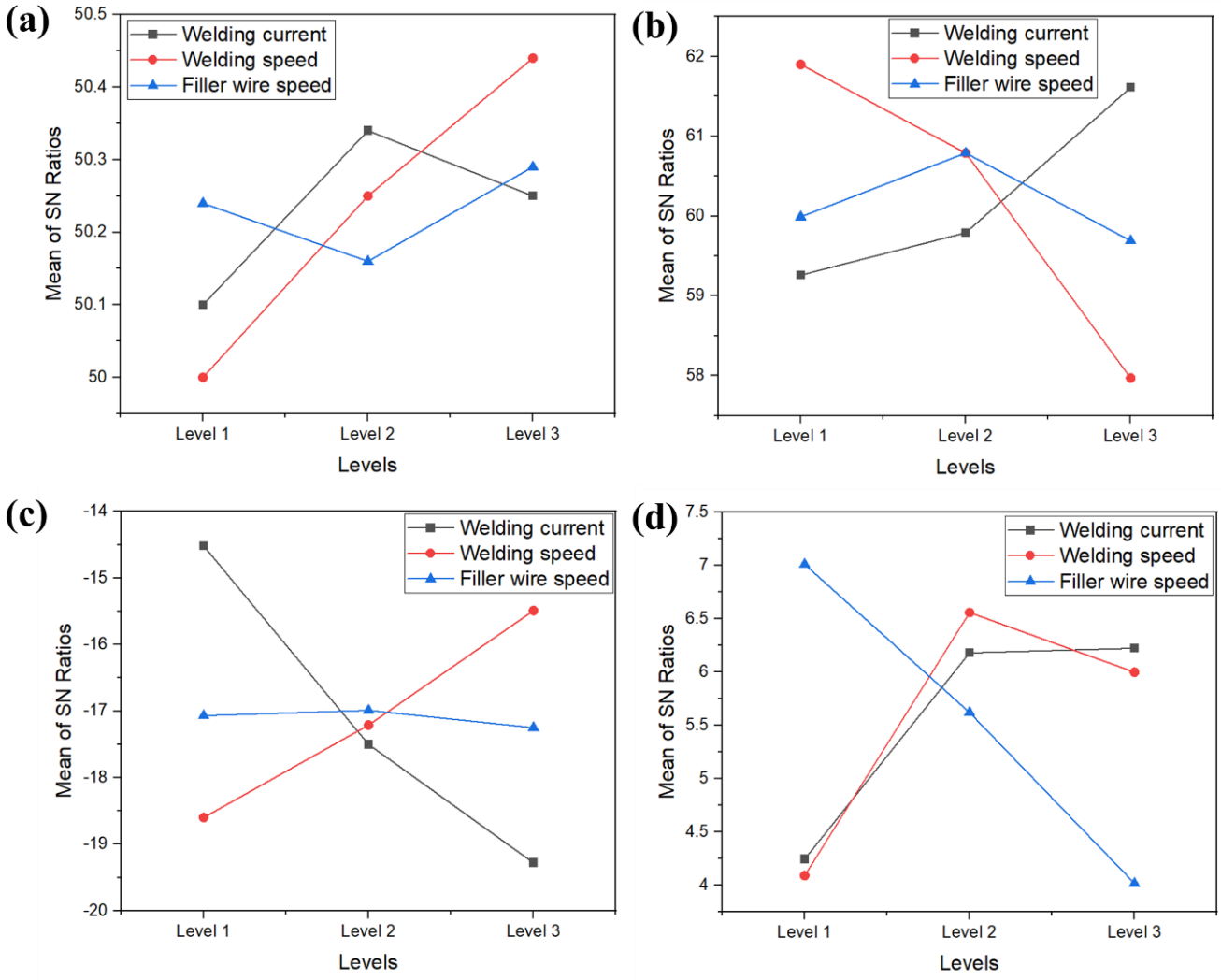

Fig. 6: Main effects plot of S/N ratios (a) hardness, (b) notch tensile strength, (c) front bead width, (d) front bead height

Table 8: S/N response table for hardness, notch tensile strength, front bead width and front bead height

Levels	Mean S/N ratios											
	Hardness			NTS			FBW			FBH		
	A	B	C	A	B	C	A	B	C	A	B	C
1	50.10	50.00	50.24	59.26	61.90	59.99	-14.52	-18.60	-17.07	4.243	4.089	7.011
2	50.34	50.25	50.16	59.79	60.79	60.79	-17.50	-17.21	-16.99	6.180	6.559	5.620
3	50.25	50.44	50.29	61.61	57.97	59.69	-19.28	-15.49	-17.25	6.223	5.998	4.015
Delta Δ	0.24	0.44	0.13	2.35	3.93	1.28	4.71	3.11	0.26	1.981	2.470	2.996
Rank	2	1	3	2	1	3	1	2	3	3	2	1

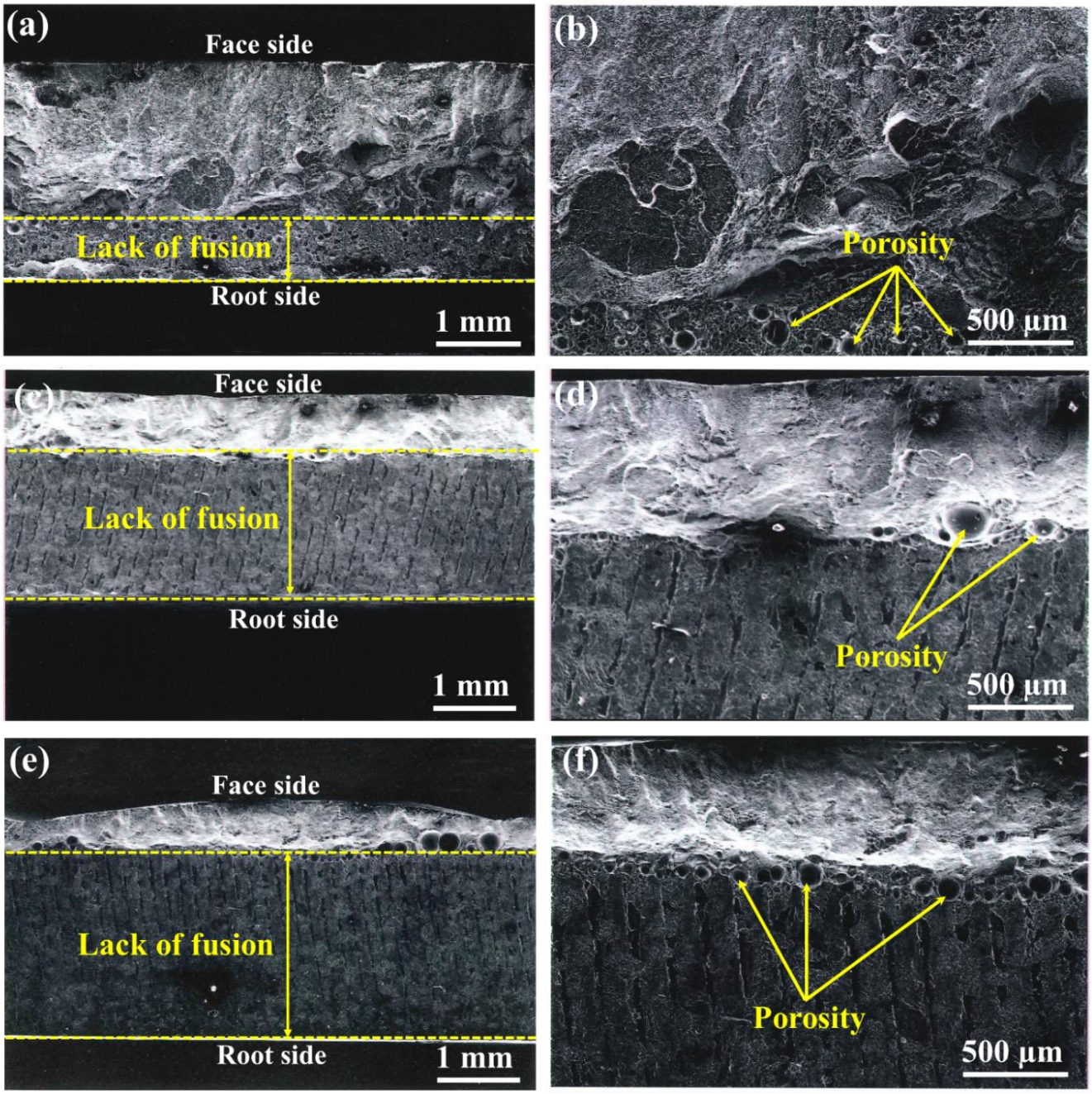

Fig. 7: SEM microstructure of fracture surfaces of notch tensile specimens, a) Specimen-1 at 20X lack of penetration(LOP) observed at root side; b) at 50 X porosity observed in root area initiation predominantly transgragular fracture observed in specimen 1; c) specimen-2 at 20X; lack of penetration observed at weld area; d) at 50 X brittle and ductile fracture observed; e) specimen-3 at 20X; lack of penetration observed root to face section, and predominantly brittle fracture with no shear region observed f) at 50 X porosity observed at edge of reinforcement and LOP

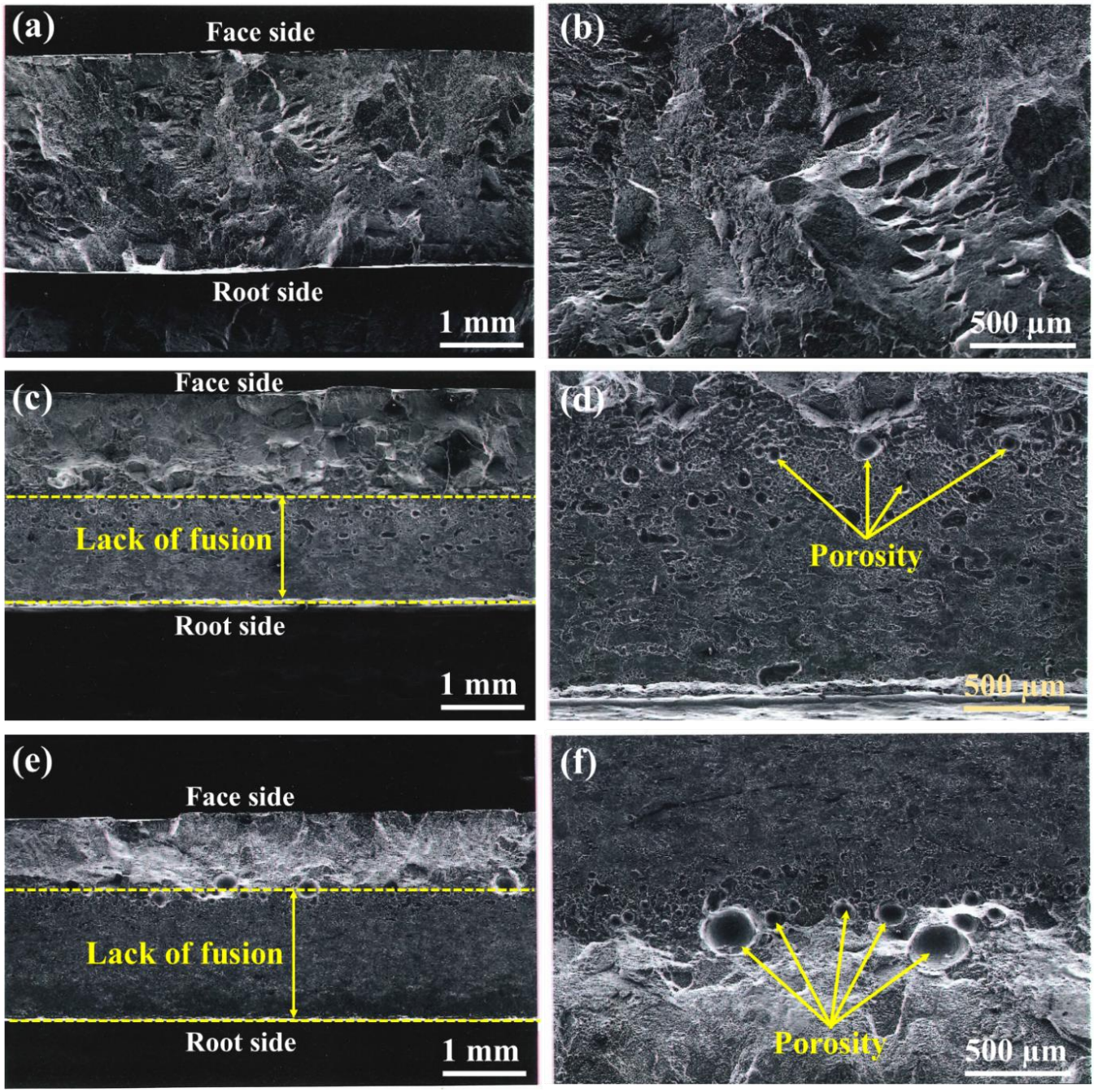

Figure 8: SEM microstructure of fracture surfaces of notch tensile specimens, a) specimen-4 at 20X no lack of penetration observed, predominantly ductile fracture with shear region; b) at 50 X; c) specimen-5 at 20X; lack of penetration and porosity observed at root area d) at 50 X; e) specimen-6 at 20X; lack of penetration observed in the weld area, brittle fracture observed, f) specimen no. 6 at 50 X

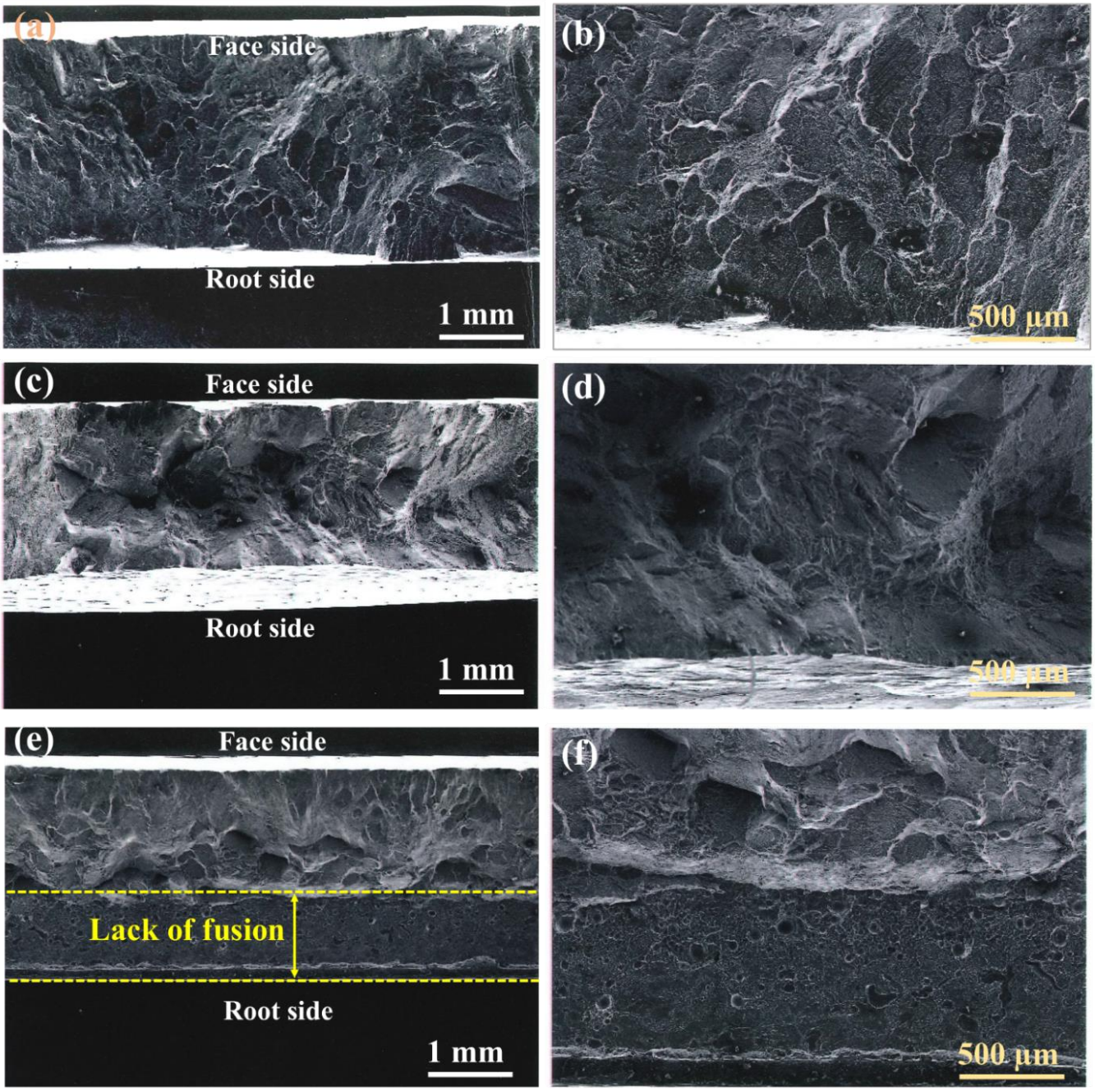

Fig. 9: SEM microstructure of fracture surfaces of notch tensile specimens, a) specimen-7 at 20X, no lack of penetration observed, predominantly ductile fracture with shear fracture region observed; b) at 50 X; c) specimen-8 at 20X, similar fracture like specimen no 7 observed; d) at 50X; e) specimen-9 at 20X; lack of penetration observed in the root area, mixed fracture observed; b) at 50 X.

Table 9: ANOVA - Weld hardness- HV

Factors	Degree of freedom (dof)	Sum of squares (SS)	Mean square MS	F-value	P-value	Contribution%
A	2	124.20	62.10	28.88	0.033	21.98
B	2	402.9	201.4	93.70	0.010	71.32
C	2	33.60	16.80	7.81	0.133	5.95
Error	2	4.30	2.15	--		0.76
Total	8	564.90				

Table 10: ANOVA - Notch tensile strength

Factors	Degree of freedom (dof)	Sum of squares (SS)	Mean square MS	F-value	P-value	Contribution%
A	2	112098	56049	8.091	0.110	25.53
B	2	289936	144968	20.929	0.045	66.03
C	2	23195	11597	1.6743	0.374	5.29
Error	2	13853	--	--		3.15
Total	8	439082				

Table 11: ANOVA- Front bead width

Factors	Degree of freedom (dof)	Sum of squares (SS)	Mean square MS	F-value	P-value	Contribution%
A	2	23.81	11.91	41.05	0.023	66.37
B	2	10.85	5.43	18.70	0.050	30.24
C	2	0.64	0.32	1.10	0.470	1.77
Error	2	0.58	0.29	--	--	1.62
Total	8	35.88				

Table -12: ANOAV- front bead height

Factors	Degree of freedom (dof)	Sum of squares (SS)	Mean square MS	F-value	P-value	Contribution%
A	2	0.0266	0.0133	14.77	0.063	23.33
B	2	0.0362	0.0181	20.11	0.047	31.75
C	2	0.0494	0.0247	27.44	0.035	43.35
Error	2	0.0018	0.0009	--	--	1.57
Total	8	0.1140				

The results of ANOVA for front bead width presented in Table 11 indicates that welding current (A) is the most prominent factor followed by welding speed, while filler wire rate has almost no effect.

Prediction for optimized value and confirmation test

Experimental verification is the final stage of Taguchi's design. The output response of predicted values and experimental values was compared for the confirmation of experiment. The predicted value of S/N ratio for hardness can be calculated by using Eq. 7. [32-34].

$$S/N_{predicted} = S/N_m + \{(S/N_{A2}-S/N_m) + (S/N_{B3}-S/N_m) + (S/N_{C3}-S/N_m)\} \quad \text{Eq. 7}$$

Where, S/Nm is the overall mean S/N ratio and S/NA2, S/NB3 S/NC3 are the mean S/N ratio at optimal level of factors, in case of hardness the overall mean S/N ratio is about 50.23. S/N ratios for optimal levels A2, B3 and C3 obtained from Table-8 are 50.34, 50.44 and 50.29 respectively. By using these values, the predicted S/N can be calculated by using Eq.7.

$$S/N\ predicted = 50.23 + \{(50.34-50.23) + (50.44-50.23) + (50.29-50.23)\} = 50.61$$

The corresponding value of hardness can be calculated from Eq.1 ($50.61 = -10 \log (y^2)$), the predicted value of hardness is around 341 HV,

For confirmation, 2 x plates were welded according to optimum optimal levels (A2B3C3, i.e. welding current 125A, welding speed 400 mm/min and filler wire speed 350 mm/min). The hardness was measured at weld bead area, and average hardness of these experiments was found to be 335HV. This result is very close to predicted result. Table-13 shows comparison of predicted hardness with experimental results.

Table-13: Results of confirmation experiments and predicted values of hardness

Factors			Output parameters or response				
A	B	C	Predicted		Experimental		Error%
			HV	S/N	HV	S/N	
125	400	350	341	50.61	335	50.5	1.75

Conclusion:

In this paper, Taguchi's design of experiments (L9) was used to optimize the effect of tungsten inert gas welding parameters on weld hardness, notch tensile strength and weld bead geometry of 2.0 mm Ti6Al4V titanium alloy. The factors considered were welding current, welding speed and filler wire speed. It is found that weld hardness depends on both welding current and welding speed parameters, and as the welding current increases from 100 to 150 amps, the value of hardness increases then decreases. Based on S/N ratio, the optimal welding parameters for weld hardness (larger is the better) are welding current at level-2 (125 amps), welding speed at level-3 (400 mm/min) and filler wire speed at level-3 (350 mm/min). ANOVA results presented in table-9, reveals that welding speed has a major influence on weld bead hardness with contribution of about 71.32 %, followed by welding current and filler wire speed.

Based on the S/N ratio, optimal welding parameters for notch tensile strength are A3B1C2, the welding current at level-3 (150 amps), welding speed at level -1 (200 mm/min) and the filler wire speed at level-2 (350 mm/min). From analysis of variance results tabulated in table-10, welding speed proved to be the most influential factor having contribution of about 66.03%, followed by welding current with contribution about 25.53%.

Based on the S/N ratio, optimal parameters for front bead width are the welding current at level-1 (100 amps), welding speed at level -3 (400 mm/min) and the filler wire speed at level-2 (350 mm/min). From analysis of variance results, welding current proved to be the most influential factor having contribution of about 66.37%, followed by welding speed with contribution about 30.26%. Filler wire speed had little or no contribution towards front bead width as the P value is more than 0.05.S/N ratios and ANOVA results for front bead height showed that filler wire speed is the most influential factor with percent contribution of about 43.33%, followed by welding speed and welding current. The confirmation test was carried out at optimal working conditions, predicted and observed values of hardness was close to each other with an error of about 1.75%.

References

1. Li R, Li Z, Zhu Y, et al. A comparative study of laser beam welding and laser–MIG hybrid welding of Ti–Al–Zr–Fe titanium alloy. Materials Science and Engineering: A. 2011;528(3):1138-1142.
2. Balasubramanian T, Balakrishnan M, Balasubramanian V, et al. Influence of welding processes on microstructure, tensile and impact properties of Ti-6Al-4V alloy joints. Transactions of Nonferrous Metals Society of China. 2011;21(6):1253-1262.
3. Casalino G, Mortello M, Campanelli SL. Ytterbium fiber laser welding of Ti6Al4V alloy. Journal of Manufacturing Processes. 2015;20:250-256.
4. Veiga C, Davim J, Loureiro A. Properties and applications of titanium alloys: a brief review. Rev Adv Mater Sci. 2012;32(2):133-148.
5. Short A. Gas tungsten arc welding of α+ β titanium alloys: a review. Materials Science and Technology. 2009;25(3):309-324.
6. Liu H, Wang H, Zhang Z, et al. Enhancing the mechanical properties of electron beam welded TC17 titanium alloy joint by post-weld heat treatment. Journal of Alloys and Compounds. 2019;810:151937.
7. Cheng M, Yu B, Guo R, et al. Electron beam welding of a novel near α high temperature titanium alloy powder compact: Effect of post-welding heat treatment on tensile properties. Journal of Materials Research and Technology. 2021;10:153-163.
8. Prasad S, Monaco Jr EA. Repairing an implant titanium milled framework using laser welding technology: a clinical report. The Journal of prosthetic dentistry. 2009;101(4):221-225.
9. Yunlian Q, Ju D, Quan H, et al. Electron beam welding, laser beam welding and gas tungsten arc welding of titanium sheet. Materials Science and Engineering: A. 2000;280(1):177-181.
10. Quazi M, Ishak M, Fazal M, et al. Current research and development status of dissimilar materials laser welding of titanium and its alloys. Optics & Laser Technology. 2020;126:106090.
11. Balasubramanian M. Prediction of optimum weld pool geometry of PCTIG welded titanium alloy using statistical design. Engineering Science and Technology, an International Journal. 2016;19(1):15-21.
12. Balasubramanian M, Jayabalan V, Balasubramanian V. Effect of microstructure on impact toughness of pulsed current GTA welded α–β titanium alloy. Materials Letters. 2008;62(6-7):1102-1106.
13. Huda N, Kim JW, Ji C, et al. Determination of Optimal Weld Parameter for Joining Titanium Alloys by Gas Tungsten Arc Welding using Taguchi Method. Journal of Welding and Joining. 2021;39(1):81-88.
14. Akbari M, Saedodin S, Toghraie D, et al. Experimental and numerical investigation of temperature distribution and melt pool geometry during pulsed laser welding of Ti6Al4V alloy. Optics & Laser Technology. 2014;59:52-59.
15. Omoniyi P, Mahamood R, Arthur N, et al. Laser butt welding of thin Ti6Al4V sheets: Effects of welding parameters. Journal of Composites Science. 2021;5(9):246.
16. Balasubramanian M, Jayabalan V, Balasubramanian V. Process parameter optimization of the pulsed current argon tungsten arc welding of titanium alloy. Journal of Materials Science and Technology. 2008;24(3):423-426.
17. Khatter A, Kumar P, Kumar M. Optimization of Process Parameter in TIG Welding Using Taguchi of Stainless

Steel-304. International Journal of Research in Mechanical Engineering and Technology. 2014 2014;4:31-36.
18. Juang S, Tarng Y. Process parameter selection for optimizing the weld pool geometry in the tungsten inert gas welding of stainless steel. Journal of materials processing technology. 2002;122(1):33-37.
19. Pasupathy J, Ravisankar V. Parametric optimization of TIG welding parameters using taguchi method for dissimilar joint (Low carbon steel with AA1050). Journal of Scientific & Engineering Research. 2013;4:25-28.
20. Dongxia Y, Xiaoyan L, Dingyong H, et al. Optimization of weld bead geometry in laser welding with filler wire process using Taguchi's approach. Optics and Laser Technology. 2012;44(7):2020-2025.
21. Gauri SK, Chakraborty S. Multi-response optimisation of WEDM process using principal component analysis. The International Journal of Advanced Manufacturing Technology. 2009;41(7):741-748.
22. Naik AB, Reddy AC. Optimization of tensile strength in TIG welding using the Taguchi method and analysis of variance (ANOVA). Thermal Science and Engineering Progress. 2018;8:327-339.
23. Vankanti VK, Ganta V. Optimization of process parameters in drilling of GFRP composite using Taguchi method. Journal of Materials Research and Technology. 2014;3(1):35-41.
24. Tugrul Ogulata R, Mavruz Mezarcioz S. Optimization of air permeability of knitted fabrics with the Taguchi approach. The Journal of the Textile Institute. 2011;102(5):395-404.
25. Anoop C, Kumar P. Application of Taguchi methods and ANOVA in GTAW process parameters optimization for aluminium alloy 7039. International journal of engineering and innovative technology (IJEIT). 2013;2(11):54-58.
26. Rao SR, Padmanabhan G. Optimization of machining parameters in ECM of Al/B4C composites using Taguchi method. International Journal of Applied Science and Engineering. 2014;12(2):87-97.
27. Kirby ED, Zhang Z, Chen JC, et al. Optimizing surface finish in a turning operation using the Taguchi parameter design method. The International Journal of Advanced Manufacturing Technology. 2006;30(11):1021-1029.
28. Yang Wp, Tarng Y. Design optimization of cutting parameters for turning operations based on the Taguchi method. Journal of materials processing technology. 1998;84(1-3):122-129.
29. Baig MM, Mohiuddin A, Akram M, et al. Optimization of Tig Welding Parameters for Hardness and Study the Effect on Microstructure of Titanium Alloy. GRD Journal for Engineering.2(4):23-30.
30. Mooli H, Seeram SR, Goteti S, et al. Optimal weld bead profiles in the conduction mode LBW of thin Ti–6Al–4V alloy sheets. AIMS Materials Science. 2021;8(5):698-715.
31. Kar P, Behera J, Pradhan J, et al. Parametric Optimization and Taguchi Application of bead geometry and HAZ width in submerged arc welding using a mixture of fresh flux and fused flux. International Journal of Research in Engineering and Science.6(5):79-91.
32. Do Kim K, Choi DW, Choa Y-H, et al. Optimization of parameters for the synthesis of zinc oxide nanoparticles by Taguchi robust design method. Colloids and Surfaces A: Physicochemical and Engineering Aspects. 2007;311(1-3):170-173.
33. Kumar S, Balachander S. Studying the effect of reinforcement parameters on the mechanical properties of natural fibre-woven composites by Taguchi method. Journal of Industrial Textiles. 2020;50(2):133-148.
34. Babu J, Philip J. Experimental studies on effect of process parameters on delamination in drilling GFRP composites using Taguchi method. Procedia materials science. 2014;6:1131-1142.